Research Article

Preparation, Characterization, Properties and Applications of Lead Zerconate Titanate Thin Films: A Review

Vipin Patait[1] and T. K. Mandal[2*]

[1]Samrat Ashok Technological Institute, Civil Line, Vidisha, M.P, India
[2]ICFAI Tech School, ICFAI University
Rajawala Road, Central Hope Town, Selaqui, Dehradun-248011, India

Article History: Received: 11 January 2021; Revised: 12 February 2021; Accepted: 27 March 2021; Published online: 16 April 2021

Abstract: Lead Zerconate Titanate (PZT) thin film has been extensively investigated for the various important applications. Sol-gel method, chemical vapour deposition (CVD), sputtering method, pulsed laser deposition (PLD), chemical solution deposition (CSD) and ink jet method have been reviewed. Different characterization methods like X-Ray Diffraction (XRD), Scanning Electron Microscopy (SEM), Energy Dispersive X-Ray Analysis (EDX) and Transmission Electron Microscopy (TEM) for the as prepared PZT thin film have been studied. Important applications of PZT thin film as sensor, transducers and in MEMS has been addressed in this review. Energy harvesting applications of PZT thin film has also been focused.

Keywords: Fabrication, PZT thin film, Energy harvesting.

1. Introduction

Lead Zerconate Titanate (PZT) being the piezoelectric material has got the dual nature i.e. when experiencing force across the surface, it will generate the potential and when experiencing electric field across the surface will generate the force in a particular direction. It is the most significant material has been used for various scientific applications due to its inherent piezoelectric and ferroelectric properties [1][2][3][4]. With the incorporation of new methods of fabrication and characterization, PZT has been explored in various domains. The different methods of fabrication allow the researcher to select the apt one to get the desirable outcome, i.e. to get the damage information of the surface [5], to develop the flexible electronics devices [6], to develop the single crystal structure on a given substrate which ultimately would have the better piezoelectric properties [7], and to create the touch based devices for better user interface [8]. Varied combination of Zr/Ti ratio provides PZT the desirable morphotropic phase boundary (MPB) [9]. PZT has been doped with different materials to have the better morphology which incidentally enhances its properties even in non MPB phase [10], doping with Fe^{3+} decreases the ferroelectric polarization but increases the magnetization and provides multifunctional behavior to PZT [11], doping with La, Nb and Fe does the variation in the lattice structure which is required to enhance the one and more properties of the PZT [12]. $Bi_{3.25}La_{0.75}Ti_3O_{12}$ (BLT) as a buffer layer in varied thicknesses is used with PZT to provide it a multilayer facet and gives it desirable orientation (1 1 1 or 1 1 0) to have better ferroelectric properties [13]. Multi-coating of PZT improves the micro level structure, its orientation and also enhances the properties [14]. Crystal information and composition of PZT can be collected by the X-ray photoelectron spectroscopy (XPS) [15]. The inherent properties of the PZT can be protected by the utilization of the protective layer [16], $0.67Pb(Mg_{1/3}Nb_{2/3})O_3$-$0.33PbTiO_3$/$Pb(Zr_{0.52}Ti_{0.48})O_3$ (PMN-PT/PZT) heterostructures are the high performance structure as the number of interfaces increases [17]. During the course of synthesis the PZT thin film forms the capacitive structure and that makes its utilization as memory storage device [18][19]. Study of temperature effect on PZT shows that it is a good candidate for the development of electronic device at high and a low temperature [20][21], and study on working pressure shows that it changes the crystalline structure and morphology of the PZT [22]. When PZT is put under stress its properties remain intact at the low stress, but cracks developed inside the structure and it increase the dielectric loss with the increase in stress[23], initial stress shows that the Lamb and SH wave propagates swiftly through the PZT [24]. Sometimes the small amount of stress onto the surface of thin film may result in total damage of it, but controlled stress method can take care of it[25].

The objective of this paper is to thoroughly investigate the various methods available to fabricate the PZT thin film with the combination of different materials so as to get the better information of the PZT lattice structure. The impact of different combinations of the material used to fabricate during the process and after the process have also been investigated. In the later part of the paper piezoelectric, ferroelectric and other significant properties of the PZT material have been discussed which would lead to its effective utilization as a dominant material for various applications. And finally the utilization of the PZT in various possible applications has been described.

The following segment will provide more insight on the methods used for the fabrication of PZT thin film and modification adopted in those methods over the years.

2. Fabrication Methods

PZT thin film materials have been prepared utilizing several methods. Some of the methods are presented in Figure. 1.

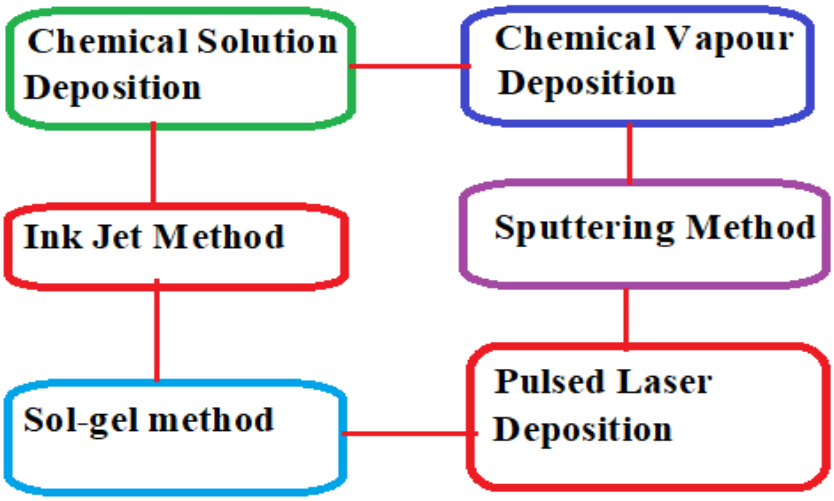

Figure .1. Different preparation methods of PZT thin films

2.1. Sol-gel method

The traditional sol-gel method utilizes the metal organic precursor as the source material for the fabrication process. These precursor then spin coated onto the substrate which is followed by drying and annealing process to get the finished thin film of PZT. As per the available research modification took place at each and every stage of it to get the best of PZT thin film. These modifications includes the different ratio of the base metal solution, different solvents, substrate material, substrate temperature, spin coating speed, temperature of drying process, gases involved in drying process, annealing temperature, annealing process and analysis methods. Based up on this we are presenting the account of key research done in this area.

Aiying Wu et. al. [25]utilized the sol gel method to make the PZT thin film on Al substrate. Different chemicals are used to get the stable sol for longer period. Seeding effect, where the pure PZT powder is mixed in different ratios to the parent sol is also analysed to get the better perovskite structure. Lead acetate trihydrate, zirconium tetra-n-propoxide, zirconium acetylacetonate, titanium tetra-isopropoxide, titanium diisopropoxide bis (2,4-pentanedionate) were used as the initial reagents. These reagents are mixed with the alcoholic medium with various stabilizers to get the stable precursor. Ethanol, acetone, ethylene glycol, propanol, 1,2-propanediol and ethanolamine are used to dilute the PZT precursor sol. The film is prepared by dip coating method on Al substrate. The film is dried at 120^0C for 30 minutes and fired at around 700^0C for 1 hour. XRD and Scanning Electron Microscope (SEM) analysis shows that with the use of seed at 5% wt. the temperature at which the perovskite structure is obtained has come down. Oleg Babushkin et. al. [26] studied X-Ray diffraction of PZT thin film and finding out the crystallisation of isotherms with respect to time. SiO_2, Ti and Pt with the thickness of 1 µm, 1 nm and 10 nm respectively are taken with silicon substrate. Precursor prepared by sol gel method is deposited by the spin coating method. The thickness of this is monitored by the repetition of spin coating. Pyrolysis performed at 350^0C. High temperature XRD is adopted to study the thin film crystallisation. A furnace is designed for this. SEM characterisation is also done of the microstructure of the thin film after each heat treatment. The XRD analysis shows that the presence of halo transformed due to isothermal treatment. Q. Zou et. al. [27] fabricated PZT thin film at low temperature on $Pt/Ti/SiO_2/Si$ substrate by sol gel method used noval polyol metalorganic route. Differential thermal analysis (DTA), thermogravimetric analysis (TGA), Fourier transform infrared (FTIR), and X-ray diffraction is performed for analysis purpose. Glycolate sol is used to sideline the pyrolysis process. $ZrCl_4$ and $TiCl_4$ in 1,2-*n*-propandiol(pro-pylene glycol) gives Zr and Ti sols. Lead acetate [$Pb(CH_3\ COO)_2$] was added in Ti and Zr to get further solution. By product $PbCl_2$ is removed using filtration. Pb, Zr and Ti solutions were mixed to form Pb/Zr or Pb/Ti and they are again mixed to get $Pb(Zr_{0.52}Ti_{0.48})O_3$ pyrolysis at 350 – 400^0C and annealing at 500-600^0C comes next. TGA curve shows the weightloss of organic group from the solution at 250 – 430^0C during pyrolysis. PZT precursor heating at 730^0C indicates that the formation of PbO and decomposition of the organic by DTA analysis. At 550^0C crake free, single crystal perovskite structure using spin coating and annealing is formed. Ferroelectric properties remain intact.

Zuleeg R et. al.[28] used integrated sol gel method for the preparation PZT thin film with the different ratios of Zr/Ti are presented in this paper. Pt, Si and GaAs as substrate to be used in the non-volatile random access

memory (NVRAM). Precursor was synthesized using schlenk technique under standard atmospheric condition. A polymeric solution was prepared with the help of precursor and then spins casted on Pt, Si and GaAs. The prepared thin film is characterised by the Rutherford Backscattering (RBS), XRD, Ellipsometry and SEM. RBS is used for the stoichiometry of thin films. Ellipeometric measurement shows that the refractive index has been changed from 2.0 to 3.0. Thibault Dufay et. al. [29] fabricated PZT thin film first on Al, transferred on polymer and then Al removed to have it on polymer. Spin coating technique is used to obtain the PZT film on a substrate from the precursor as the base material. It is then heated at 650^0C to get crystalline structure. polyurethane (PU, NOA81, Norland Optics®)layer is deposited on PZT next and exposed for 2 hours for better bounding between them. polyethylene terephthalate (PET) is used to have a new substrate on the polymer. The glue is used to protect the PZT structural loss during the etching process. Iron chloride solution is used to remove Al. XRD shows the regular PZT peaks on the surface. Xing Wang et. al. [30] prepared the precursor solution first using the sol gel method and them the deposition was done. XRD, Atomic force microscopy (AFM) and SEM is performed to get phase information, surface information and interface information respectively. PZT layer on substrate fabricate by the combination of sol gel and spin coating method. It is preheated, pyrolyzed and annealed to get the desirable film. PZT film is also made by rf magnetron sputtering method where the Ar flow rate is 90sccm and pressure of the chamber is 1.5 Pa. Results show that increasing the partial pressure of oxygen in O_2/Ar converts the pyrochlore phase to pervoskit phase. AFM analysis shows that the ratio of 10/90 gives the compact and smooth surface. In SEM analysis with the same ratio provides dense and uniform structure.
Ali Shoghi et. al. [31] talks about the preparation of PZT thin film on FTO glass and finding out the optimal value of heat treatment and sol parameter in the process. Zirconium n-propoxide, titanium isopropoxide, lead acetate trihydrate, acetic acid, n-butanol, methanol, diethanolamine, and deionized Water are used in the preparation of PZT. Deep coating method with the withdrawal speed of 30 mm/Min is used for depositing PZT on FTO glass substrate. The characterization of crystal structure of the film is done by XRD, surface morphology by field emission scanning electron microscopy, roughness and homogeneity by atomic force microscopy (AFM), atomic bands and sol reactions by fourier transform infrared (FTIR), with slight pyrochlore phase 600^0c for 5 min is the optimal condition for fabrication of PZT on FTO glass. Jian He et.al. [32] PZT thin film is fabricated using sol gel method on sapphire substrate and then transferred on a flexible polyimide (PI) substrate using spalling method. XRD and raman spectroscopy is used for the analysis purpose and ferroelctric properties are also analysed. Lead acetate trihydrate dissolved in acetic acidwith a 10% excess of Pb at 115^0C. It is added to mixture of zirconium propoxide and titanium isopropoxide, distilled water and ethylene glycol is added then to save it from cracking. Finally a PZT precursor is made after 24 h waiting and filtering. This precursor is spin coated at 500 rpm for 6 s and 3000 rpm for 20 s. Pyrolyzed at 350^0C for 10min for removing the organics and annealed at 650^0C for 10min to crystallize. This process is reported for 20 times to obtain the film. It is annealed again at 650^0C for 30 min. Au-100 nm/Cr-20 nm layer is grown on it using magnetron sputtering process. Ni stressor layer is electroplasted on it. Then spalling process is performed. With this we have PZT on Ni substrate. The top electrode is placed on PZT and then it is attached to PI substrate. XRD shows the diffraction peaks of the PZT on Ni layer is almost same as it was on sapphire substrate . Raman spectra shows that the desired perovskite structure has been achieved. SEM shows that it has clear interface with sapphire and Ni layer both. Shagun Monga et. al. [33] gave the information of the optical properties of PZT and effect of substrate selection on it. The PZT preparation is done with the Sol Gel approach. Lead acetate trihydrate dissolved in acetic acid, heated at 105^0C is then taken. zirconium n-propoxide and titanium isopropoxide in requiredratio is taken. The following solutions are taken for getting the required precursor. Ultrasonic cleaner for homogeneous solution, distilled water is used to get the required viscosity and to reduce surface tension. Spin coating technique is used to make the PZT thin films form the finally prepared solution. PZT thin film deposited on corning glass, ITO glass and quartz. It is tested for optical properties by XRD, Raman and UV-Vis spectroscopy. XRD shows the provskite structure at 650^0C, raman spectroscopy shows the presence of tetragonal phase, and UV-vis spectroscopy shows the different values of absorbance, reflectance and transmittance when different substrates are used. Xing Wang et. al. [34] Multilayer of $Pb_{1.25}(Zr_{0.52},Ti_{0.48})O_3$/ $Pb_{1.1}(Zr_{0.52},Ti_{0.48})O_3$ is fabricated on Pt/Si/ SiO_2 substrate and the effect of layers ratio on the thin film is analysed in this paper. Lead acetate trihydrate, tetrabutyl titanate, and zirconium nitrate used for the precursor preparation. Acetic acid and formamide are used to keep the pH adjusted to the desirable level. XRD and X-ray photoelectron spectroscopy (XPS) analysis was done. And the ratio of 1/3 shoed the strong result. Figure.2 shows the preparation of PZT using modified sol-gel method

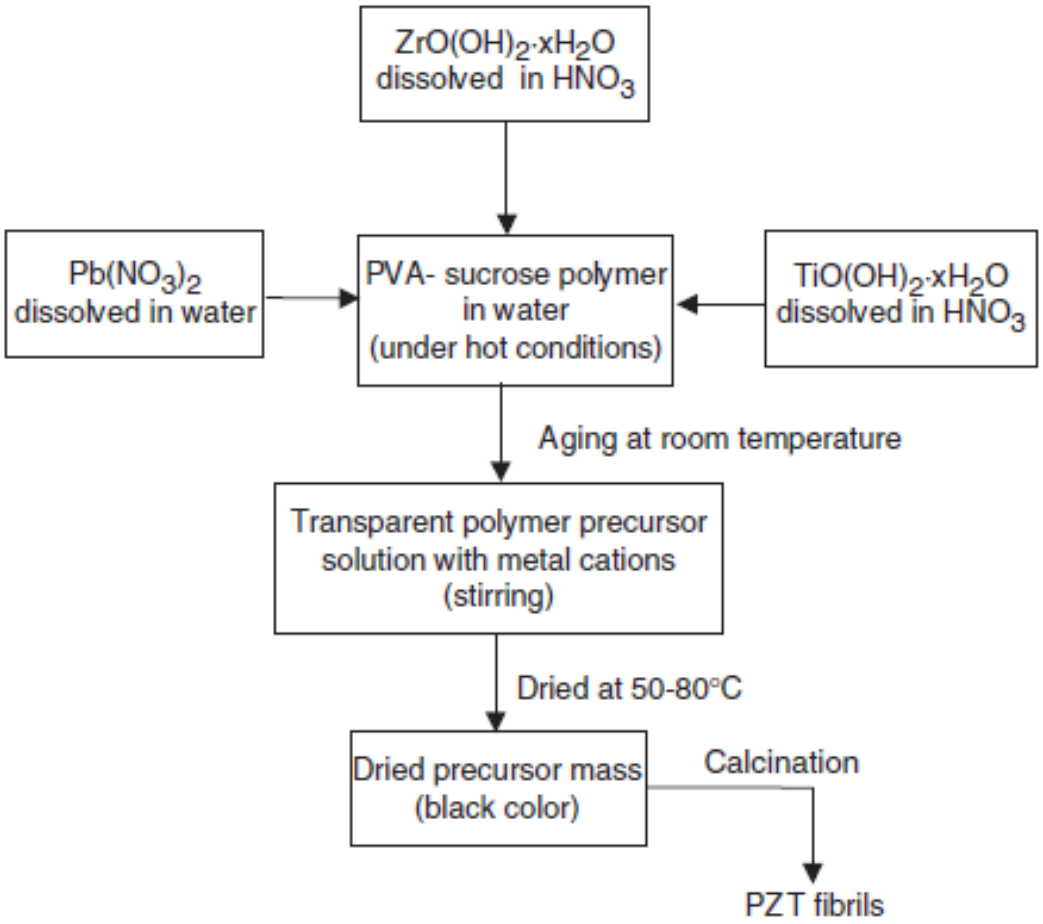

Figure.2 Preparation of PZT using modified sol-gel method **(J A Ceram Soc 2005)**

2.2. Chemical Vapour Deposition (CVD)

CVD is also one of the prominent techniques used to fabricate PZT thin film. The core of the method lies with the apparatus used in order to fabricate the film. There are several manufacturers in the field making state of the art apparatus. These apparatus consists of chambers for the metalorganic solution to place, uses inert gases and oxygen in particular at various pressure and temperature as required, chamber for sputtering to take place at controller pressure and temperature, base for substrate to place at different temperature etc. the following research gives an insight on it.

S.T. Kim et. al. [35] Used electron cyclotron resonance plasma enhanced chemical vapor deposition (ECR PECVD) method to fabricate PZT thin film with the utilization of Metal Organic (MO) source. Lead ß-diketonate ($Pb(DPM)_2$, $Pb(C_{11}H_{19}O_2)_2$), titanium iso-propoxide(TiIP, $Ti(i\text{-}OC_3H_7)_4$), zirconium t-butoxide (ZrTB, $Zr(t\text{-}OC_4H_9)_4$) is used as precursor along with O_2. Magnetron is generating 2.4 GHz radiation is introduced. Pt(70 nm) /Ti (100 nm) /SiO,(600nm)/Si substrates is used at 500^0C. The structure and the chemical composition are analysed through XRD and wavelength dispersive X-Ray spectroscopy (WDS). Chemical composition shows the ratio of Zr/Ti as 0.35, 0.57 and 0.63, whereas the thickness of the film obtained is 1100, 1000 and 900 Å. XRD shows the single phase perovskite structure obtained successfully for all of them. As the ratio of Zr/Ti increases the current density also increases. Zr/Ti ratio of 0.57 and a thickness of 1000 Å, shows the highest dielectric constant. Su Ock Chung et al. [36] fabricated PZT thin film by ECR PECVD on $Pt/Ti/SiO_2/Si$ substrate at 470^0C and 500^0C. The ECR PECVD system have discharge chamber, reaction chamber, metal organic source (MO) and pumping source. ECR generated by matching the microwave frequency with the electron frequency at 2.4 GHz. Dipivaloylmethanato lead , zirconium t-butoxide and titanium iso-propoxide used as MO source. Ar, O_2 and MO flow rate is all controlled. The substrates temperature is controlled by thermocouple. At 500^0C only perovskite peaks are found in XRD. TEM also confirms the same that 470^0Cis not enough for planer film. June-Mo Koo et. al. [37] deposited The PZT thin film using CVD technique and the effect of the purge gas on properties of PZT is analysed. Nexcap 2000 CVD reactor (Sunic System Ltd.) is used for the deposition. $Pb(tmhd)_2$, $Zr(tmhd)_2(^iOPr)_2$ and $Ti(tmhd)_2(^iOPr)_2$ is used

as precursor, film deposited on Ir/Ti electrode which is deposited on SiO_2/Si by magnetron sputtering. PZT deposition takes place at 530^0C. Purged gas used in two steps, before the PbTiO3 (PTO) deposition and PZT layer deposition. It is used to stabilize the reaction chamber. The main function of the purge gas is to stabilize the chamber at the time of supply of metalorganic precursor. At optimized purge gas flow, that is N_2/O_2 = 500/1500 sccm, PZT thin film displayed 92.2% (1 1 1)-orientation. Won Gyu Lee et. al. [38] developed PZT thin film by plasma enhanced chemical vapor deposition (PECVD) method. Compositional distribution, surface morphologies, phase structure, and electrical properties were analysed. SEM and auger electron spectroscopy (AES) is used for analysis. Pb $(C_2H_5)_4$ (TEL, 5N purity), $Zr(O\text{-}i\text{-}C_4H_9)_4$ (ZTB, 5N purity) and $Ti(O\text{-}i\text{-}C_3H_7)_4$ (TTIP, 5N purity) is used for the fabrication. An apparatus used consists of source delivery, vacuum system and cold wall reaction chamber is used. Pt/SiO2/Si substrate is used. Some parameters are set as chamber pressure 300mTorr, substrate temperature 250^0C, RF power 20W at 13.56 MHz. Annealing performed under O_2 shows no deviation in the content of Pb at 650^0C. XRD shows that the perovskite structure obtained at the temperature range of 450 – 550^0C. Gang He et al. [39] fabricated PZT thin film along with the buffer layers of $PbTiO_3$(PT) and $PbZrO_3$(PZ) by chemical vapour deposition and the surface analysis is done by XRD, SEM and AFM. Pt(1 1 1)/Ti/SiO_2/Si(1 0 0) is used a s substrate. Leadacetate $(Pb(CH_3COO)_2 \cdot 3H_2O)$, tetrabutyl titanate $(Ti(OC_4H_9)_4)$, andzirconium nitrate $(Zr(NO3)_4 \cdot 5H_2O)$ are the source and 2-methoxyethnaol $(HOCH_2CH_2OC_2H_5)$ is a solvent and glacial aceticacid (CH_3COOH) is a catalyst to control pH is used. A syringe consist of membrane filter is used to drop precursor on substrate. PT ($PbTiO_3$) solution, then the PZT-0.6 ($PbZr_{0.6}Ti_{0.4}O_3$) solution, the PZT-0.5 ($PbZr_{0.5}Ti_{0.5}O_3$) solution, and finally the PZT-0.4 ($PbZr_{0.4}Ti_{0.6}O_3$) solution used in sequential order in spin coating. The film is heated on hot plates at 500^0C and annealed at 700^0C. XRD shows that PT buffer layers play a significant role in order to obtain pure perovskite structure. SEM shows that the adhesion between the layers is very clean and sharp. AFM shows that the roughness of PZT will differ with the increase of PT buffer layer thickness. Euk Hyun Kim et. al. [40] showed that new Pb(IV) precursor were utilize to prepare PZT by Ph_4Pb, $PbCl_2$, PhMgBr. In this particular work, liquid delivery metalorganic chemical deposition method is utilized because of step coverage, deposition rate uniformity and throughput (3-5). In this method the as prepared precursor is dissolved with the solvent and then it is injected into a flash evaporator. With this, the film is deposited onto the surface. In this method the use of precursor is playing very important role. There are many precursor available but a special kind of precursor is required which will not change its physical and chemical properties during the course of the preparation(3-7). There are precursor which have better resistivity at low temperature and better stability in the solution such as tetraethyllead $(Pb(C_2H_5)_4)$ and Pb $(thd)_2$ (thd = 2,2,6,6-tetramethyl-3,5-heptadiketonate). Tetraphenyl lead, Ph_4Pb and diphenyl dibromo lead, Ph_2PbBr_2 were prepared first as per the available method[8-9] with little modification. diphenyl di{bis(trimethylsilyl)amide} lead, $Ph_2Pb\{N(SiCH_3)_2\}_2$ (1) and diphenyl di(2,2,6,6-tetramethyl-3,5-heptadiketonate) lead, Ph_2Pbthd_2 (2) also prepared in this method. On Si wafer TiO_2 layer is prepared first and then PZT layer is deposited using MOCVD. Pb precursor dissolved with $Ti(OiPr)_4$ and $Zr(OPr)_4$ in butyl ether and tetraglyme for the preparation of PZT.

2.3. Sputtering Method

The basic principle of the method involves the bombardment of inert gas ion on the target matter at the controlled frequency to get the sputtering of metal atoms. These atoms deposited on the substrate positioned in front of it at limited distance. The whole process performed in the closed chamber and controlled environment of pressure and temperature. Cooling water is circulated across the target material to keep the secondary radiation in control. Over the years following development took place in this method.

P. Muralt et al. [41] used the Sol gel and Sputtering method to prepare the PZT thin film and utilized in the improvement in the speed of micromotor. In sol-gel process $Pb(C_2H_4O_2)_2.3H_2O$, $Zr(OCH_2CH_2CH_3)_4$ and $Ti[OCH(CH_3)_2]_4$ precursor are used. In sputtering method three magnetron were used with metal target and gives (100) orientation. The result shows that the dielectric constant at 100 Hz in sol gel and sputtering method are 950 and 610 respectively. And dielectric losses at 100 Hz are 3% and 3.5 – 4.5% respectively. T Hata et al. [42] fabricated PZT thin film using reactive sputtering method. The target is ZrTi alloy and PbO pellets. Zr, Ti and PbO mixture is also proposed. XRD is used for analysis. R. F. diode sputtering is a non-magnetron method used here. The target is ZrTi alloy and PbO pellets. The composition for target is defined as (ZrTi + xPbO) where x represents the area ratio of target surface PbO/(SPbO+SZrTi) S_{PbO}, S_{ZrTi} are the total surface area of PbO and ZrTi respectively. Ar and O_2 gases are used in the process. The glass substrate at 190^0C is used. The dependence of deposition rate on O_2/Ar ratio and combination of x gave the solid and transparent film. X = 30% , deposition rate at higher side and gases ratio at lower side gave the transparent film. XRD shows that when x = 30% and at 450)C pure perovskite PZT is obtained. Michio Watamori et al. [43] fabricated PZT thin film using helicon sputtering method.effect of oxygen and Pb distribution on the properties(dielectric constant, hysteresis loop and crystallinity) of PZT film is examined. Helicon sputtering machine (ULVACMUE – ECO – HC) is used. Rf coil used at $1.0x10^{-3}$ Torr and base pressure is $5.0x10^{-7}$ Torr. Target is PZT powder and excess

of PbO in 20, 30 and 50%. The computer simulation was used to get the composition depth profile. Enrichment of oxygen is observed using RBS. XRD for PZT at 300^0C with 50% PbO shows pyrochlore and at 580^0C no XRD pattern observed. Xin-Shan Li et al. [44] fabricated PZT thin film with single (111) orientation perovskite phase using sputtering method. Deposition temperature and annealing temperature studied. FTS – 1CB (Osaka Vacuum) instrument is used. Targets distance is 140 mm and with the substaret the distance is 130 mm. $Pb_{1.2}Zr_{0.58}Ti_{0.42}O_x$ used as target, Pt/Ti/SiO_2/Si used as substrate at 200-500^0C. RF 700 W for 120 minutes with the ratio of O_2/Ar is 4:1. At 453–656^0C thin film is annealed. XRD shows that perovskite structure obtained when deposited at low temperature 360^0C and annealed at 606^0C. surface information shows that the lower deposition temperature and lower annealing temperature gives the favourable condition for PZT thin film. Y.C. Lin et al. [45] Prepared the PZT thin film by pulsed DC magnetron method onto the Pt/Ti/SiO2/Si substrate. Pulse frequency and duty cycle, gases ratio are analysed to get better crystalline structure. Pb:Zr:Ti = 46:22:22 ratio in metallic alloy used as a target. Bipolar pulse power with the frequency of 10 kHz – 100 kHz and duty cycle of 75% - 95% is used. Deposition and annealing temperature is 100^0 C and 750^0 C. Sputtering was performed in the background pressure of $5x10^{-6}$ mbar and the working pressure of $5x10^{-3}$ mbar and the distance between target and the substrate is 60mm. Annealing process takes place at 20^0C/s. results shows when the sputtering power and temperature increase the surface don't get unstable and melted. Increase in pulse width results in linear deposition rate and lower pulse rate results in perovslite phase at duty cycle 90% and O_2/Ar ratio as 1:1. K.K. Maurya et al. [46] fabrication of PZT thin film by RF magnetron sputtering on Pt/TiO2/SiO2/Si(100). Cross Sectional Transmission Electron Microscopy (XTEM) and XRD used for the analysis purpose. Inostek Inc., Korea made RF magnetor is used for sputtering. Pt(150nm)/TiO2(20nm)/SiO2(300nm)/(100)Si(675μm) substrate at 275^0C is used. Pb1.1(Zr0.52Ti0.48)O3 ceramic used as target PZT. 5 x 10^{-4} Pa as base pressure and Ar/O_2 ratio is 80/20. 20 rpm substrate rotation speed is used. The distance between target and substrate is 110 mm. PZT film annealed at 650^0C. For the thickness range of 500nm the sputtering pressure of 4.5 Pa perovskite structure is obtained. XTEM shows the porosity at nano scale at the interface. Sujin Choi et al. [47] fabricated PZT thin using RF magnetron sputtering. Ar-ion sputtered depth profile performed to get surface information. Various ratio of O_2 are introduced to get the surface profile using XRD. The target used is n-type Si(100), it is washed through acetone and dried by nitrogen before putting on substrate holder. Substrate is heated at 573 K and rotated by 5 rpm during the sputtering process. Pb, Zr and Ti metallic having a thickness of 2 inches are used for co sputtering and mixed with Ar and O_2 during the process. The base pressure is $2.6x10^{-6}$ Torr and working pressure is $4.5x10^{-6}$ Torr. RF power used at Pb, Zr and Ti are varied to maintain the optimum ratio in PZT thin film. Thickness and conductivity of the PZT film remain high when the O_2 ratio is at lover side. As the ratio increases the thickness and conductivity both comes down. XRD shows as the O_2 ratio increases the formed PZT is more stable. XPS shows that the amount of Pb increases as the ratio of O_2 increases. Mitra Akhtari Zavareh et al. [48] fabricated PZT thin film is using powder magnetron sputtering (PMS) method on strontium titanate and strontium ruthenate. XRD, field emission scanning electron microscopy (FESEM) and X-Ray photoelectron spectroscopy (XPS) analysis is also done. In the sputtering system Ar/O_2 is maintained at 20:1 and the chamber pressure is 0.5 Pa. sputtering powder is used at 80-100 W and deposition rate is 0.2-0.3 μm/s. the taget diameter is 8 cm and the substrate is placed 8 cm away. XRD shows that this method can produce the single crystal with the characteristics of the bulk. XPS gives the better composition and FESEM shows the better surface morphology.

2.4. Pulsed Laser Deposition (PLD)

In this method the laser beam is directed towards the target material. The target gets the sufficient energy and emits the ions, these ions then accelerated towards the substrate material and deposition of the layer takes place.

L'h. Hamedi et al. [49] fabricated PZT thin film using pulsed laser deposition technique. XRD, ECP and RHEED are used for characterization. Substrate used is $SrTiO_3$. The operating condition for PLD process is energy – 3.5 J/cm^2, frequency – 2 Hz, target substrate distance – 40 mm, substrate temperature – 500 – 560^0C and pressure is 0.5 mb. Target prepared by PbO, ZrO_2 and TiO_2 powders. Highly crystalline structure has been successfully achieved on $SrTiO_3$ substrate. Javad R. Gatabi et al. [50] used Pulsed laser deposition technique for the deposition of PZT thin film. The effect of oxygen pressure and laser fluence on PZT properties is analysed. BRUKER D8 ADVANCE XRD instrument and FEI Helios Lab 400 scanning electron microscope with EDAX capability is used in the process. $Pb_{1.1}Zr_{0.53}Ti_{0.47}O_3$ compound made by plasma materials for PZT target is used. The deposition takes place on a substrate of the thickness 2 in. and inside a chamber with the pressure of $1x10^{-10}$ mbar. 248 KrF excimer laser is used for the operation and O_2 is introduced by mass flow controller. XRD shows that PZT would have deficient Pb and Zr due to deviation of the target. EDAX shows that due to laser fluence Pb content changed abruptly and the Ti content changed in a small quantity. M. Botea et al. [51] investigated the up and down graded PZT for the relation between structure and dielectric/pyro electric properties. Pulsed laser deposition (PLD) is used for the fabrication of multilayer PZT. XRD and TEM is used

for structural analysis. Capacitancevoltage (C-V), current-voltage (I-V) and hysteresis measurements is taken for electric/ferroelectric properties. pyroelectric properties were investigated as function of frequency. PZT(80/20)/PZT(52/48)/PZT(20/80)/ strontium ruthenate (SrRuO3, SRO)/ strontium titanate (SrTiO3, STO) and PZT(20/80)/PZT(52/48)/PZT(80/20)/ strontium ruthenate (SrRuO3, SRO)/ strontium titanate (SrTiO3, STO) fabricated by PLD. The remanent polarization Pr ($\mu C/cm^2$) for SM1 is 51,74 and SM2 is 21.33. coercive field Ec (MV/m) for SM1 and SM2 are 19.66 and 53.68 respectively. leakage current density at maximum positive voltage Jmax (mA/cm^2) for SM 1 and SM2 are 0.095 and 4.31 respectively. Dielectric permittivity at 0 V before (εi) for SM1 and SM2 are 107 and 421 respectively, sweeping the DC voltage from positive to negative (ε_{0+}) for SM1 and SM2 are 191 and 420 repectively. From negative to positive (ε_{0-}) for SM1 and SM2 are 101 and 427.

2.5. Chemical Solution Deposition (CSD)

Jongchul Jeon et. al. [52] gave the information of increasing the thermal stability of PZT thin film by Dysprosium doping. The main issue with the PZT structure is the change in morpotropic phase boundary (MPB) at the higher temperature. The CSD method is used to fabricate the PZT with Dy doping to deal with the issue.
CSD precursor utilizes lead acetate trihydrate, zirconium n-propoxide, and titanium (IV) isopropoxide. Zirconium n-propoxide and titanium (IV) isopropoxide were mixed homogenously. Acetic acid was added to modify it. Distilled water and n-propanol were added to make a stable solution. Dysprosium (III) nitrate hydrate was then added to get the precursor ready. Substrate is made up of Pt coated silicon wafer. The precursor is spin coated on substrate at 250^0C, pyrolysis performed at 400^0C, and crystallisation at 650^0C. The spin coating process is repeated to get the desirable thickness of the film. Thermal stability improved by 23%. Nicolas Godard et al. [53] Fabricated the $Pb(Zr_{0.53}Ti_{0.47})O_3$PZT thin film and then deposited silver electrode on top by ink jet printing method. Piezoelectric response and polarization measurements are taken. Compared the results with sputtered Pt electrode. Platinized silicon ($Si/SiO_2/TiOx/Pt$) was used as a substrate. PZT film was fabricated using CSD. Polarization-electric field (P-E) loops were measured at 100 Hz, while permittivity electric field (ε-E) loops were measured at 1 kHz, both up to DC fields of ±500 kV cm^{-1}. Scattered pinholes are observed at the electrodes. Ferroelectric characterization of the PZT thin film with inkjet printed silver top electrodes dried at 200 ^{0}C reveals high coercive field (Ec = 190 kV cm^{-1}), low permittivity (ε = 115) and high dielectric losses (tan δ = 0.20). The coercive field was found to be strongly frequency-dependent, decreasing to Ec = 110 kV cm^{-1} at 1 Hz. further increase of the sintering temperature to 300^0C resulted in much improved values.

2.6. Ink Jet Method

Itziar Fraile et al. [54] obtained PZT film using inkjet printing method. Sintering process is also performed on it. lead, zirconium and titanium are used for organometallic compound. In order to obtain sol it has to be mixed with water vapour. Stainless steel substrate and alumina and stainless steel substrate are used in PZT nanoparticle ink and PZT precursor-based ink respectively. 43 V piezovolt and 1 KHz frequency used for drop formation. Printing is performed at room temperature. Then sample placed at hot plate at 40^0C for 30 min to remove vehicles before sintering. S.P. Bathurst et al. [55] Printed PZT thin film to be utilized with the ultrasound sensor. 2-methoxyethanol and 1-butanol and 1,2-propanediol were purchased commercially and hydrous 2-methoxyethanol and 2-ethyhexanioc acid used as solvent to make the jettable ink. Viscosity, surface tension and density of the formed solution is maintained at a desirable level. Uniform distribution size is also maintained. Piezoelectric micro machined ultrasonic transducer (pMUT) was designed and fabricated to get the performance of the PZT thin film. Light interferometer was used to get the value of deflection of pMUT. It is 700nm at 27V. this data used in mechanical model and coupling coefficient is found in the range of -75 pC/N to -95 pC/N. relative permittivity is in the range of 750-890.

Table1. Summary of different methods for thin film fabrication and their features

Method	Feature	Reference
Sol gel	• Simple method for the fabrication • Involve low cost • Based upon the solutions • Requires low temperature • Annealing is done at higher temperature	[25-33]
CVD	• High quality film • Temperature vary from 300^0C to 800^0C	[34-39]
Sputtering	• Low deposition temperature • Low annealing temperature	[40-47]

	• Better oriented pervoskit structure • RF sputtering, DC sputtering, microwave sputtering etc. • Inert gases utilized	
PLD	• High powered laser pulses • Substrate temperature at higher side • Good crystalline structure • Deposition temperature has wider range	[48-50]
CSD	• Higher thermal stability • Better MPB • Solution based method	[51-52]
Ink jet	• Uniform solute distribution • Better control over the morphology • Reducing manufacturing cost	[53-54]

3. Characterization and Properties

The following table provides the information on characterisation of the material and their properties.

Table 2: Characterization and Properties of PZT

S. No.	Characterization	Properties	Reference
1	XRD shows better orientation along (2 0 0), Atomic Force Microscopy (AFM) shows minute roughness, pre polarization by negative voltage	Improved piezoelectric properties, decreased dielectric constant and ferroelectric properties	Dongdong Gong et al. [56]
2	XRD shows all layers have perovskite structure. Ti orientation transferred from 1 0 0 to 1 1 1.	Dielectric properties are ε = 1224.25 (100 Hz), ferroelectricity with a 2Pr of 40.5 μC/cm^2 and 2Ec of 108 kV/cm, and a J = 4.57×10^{-7} A/cm^2 (Ti/Pt sputtering power = 12.5 W/150 W)	Xing Wang et al. [57]
3	Thermal Expansion Coefficient (TEC) is calculated	Dielectric constant, tunability and d_{33} decreases with increasing values of TEC	Hanting Dong et al [58]
4	XRD shows the phase purity and decrease in crystalline size due to increased concentration. Raman spectroscopy shows presence of tensile strain	ferroelectric properties of the PZT film by embedding it in PMMA	K. Thanigai Arul et al [59]
5	PZT shows the fatigue at higher bipolar electric field, energy storage degraded in PZ film and PZLT film shows the better performance with fatigue free in energy storage and polarization	Energy storage performance and polarization properties of ferroelectric (FE)	Minh D et al [60]
6	XRD shows the perovskite structure but incorporation of nitrogen ions, P-E loop analysis shows that at 1.5% Co better curve is obtained and incorporation of nitrogen ions thins the curve and give lower saturation value	Shift in ferroelectric properties.	Benya Cherdhirunkorn et al. [61]
7	XRD shows the 1 1 1 orientation.	Ti rich PZT gives the perovskite structure. Properties of PZT on GaN depends on composite	Lin Li et al. [62]
8	SEM shows no cracks and for LNO substrate and the grain size is high. The current characteristics of Pt/PZT/Au, Pt/PZT/LNO, LNO/PZT/Au, and LNO/PZT/LNO	Metal oxide electrode/PZT interface shows a higher switching current than metal/PZT due to the deficiency of oxygen formed in the dead layer, the external maximum	Qicheng Zhang et al. [63]

	capacitors shows that the non-switching current increases slowly as voltage decreases from (negative) maximum to (negative) coercive voltage	voltage due to peak voltage changes regularly.	
9	AFM shows good crystallinity	good ferroelectricity and switching performance at various temperatures	Xi Chen et al. [63]
10	XRD shows the perovskite phase for PZT, no shift of diffraction angle in PLZT and shift in PLYZT due to tensile stress. Raman spectroscopy shows the peak shift towards lower frequency in PLZT and PLYZT.	The degradation in the polarization value is due to leaky nature of PZT film causes due to less nucleation center at PZT/Pt interface.	Antony Jeyaseelan A et al. [39]
11	XRD and TEM shows that the shows that the use of mica as a substrate for PZT gives the strain free film as compared to use of Si as a substrate material.		X. Er et al. [65]

4. Application

Mohan K. Bhattarai et al [64] showed the application in energy storage capacitor due to High breakdown strength, larger dielectric constant and excellent estimated energy density ~54 J/cm3 with efficiency ~70% of our thin films. Hengyang Mao et al. [65]Dilatometer gives the information of shrinkage of porous Ti and PZT. The lower value of Ti permenace shows that dense porous structure. Thermal mismatch occure between PZT and Ti at 650^0Cand cracking starts beyond 700^0C. PZT interaction with TiO_2 gives interfacial strength. with an AV of 60 V, the permeance became stationary at 92% of the initial value.. Haoran Wang et al. [66] shoed the application as transducer through DOE analysis of the experimental data, an optimal recipe is identified as the volumeratio of HBF4:H2O=1:10 at 23◦C. Min Chul Chun et al. [67]Perovsite (1 1 1) present in all 3 sample but pyrochlore (2 2 2) is also present in the samples except in where Pb is 20% in excess. Non uniform structure is also found in the other samples. Among the structures with different electrodes (Y, Al and Au) the PZT 1.2 structure with Al electrodes shows better P-V characteristics. Non noble metal shows assymetric hysteresis loop. It shows the better application in non-volatile meory. Shivaji H. Wankhade et al. [68] presented the application as energy harvester by device produces output voltage of 55 V and output power density of 36 $\mu W/cm^{-2}$. Negar Chamankar et al. [69] with Dielectric constant (ε), piezoelectric coefficient (d), and figure of merit (d×g) for PVDF-PZT nanocomposite with 0.011 PZT volume fraction were 37.29, 10.51 pCN^{-1}, and $33.46\times10^{-16}m^2/N$, respectively, and increased to 104.81, 22.93 pCN^{-1}, and 56.68 $\times10^{-16}m^2/N$ for PVDFPZT nanocomposite fibers with a volume fraction of 0.37. Masoud Rezaei et al. [70]Introduced the novel wake galloping energy harvester. It provides the broadband flow base for energy conversion. Four bimorph cantilever beam structure is placed downstream through the wind flow to check the response. It get the sinusoidal signal at the tip of the cantilever and produce the vortex. The nonlinear partial differential equations are derived and ordinary differential equations are also obtained. Yun Lu et al. [71] investigated the PZT/Ni unimorph structure which has Nd magnetic tip mass. The proposed cantilever is used to harvest the low frequency signal for wireless sensor application. The maximum power density is 270 $\mu W/cm^3$ at 50 Hz. It can switch on 10 LED without any power storage. Weijie Li et al. [72]Proposed a new method to monitor the corrosion using smart corrosion coupon (SCC) which is based on PZT patch. it utilizes the electromechanical impedance (EMI) technique for measurement. Due to corrosion the thickness of SCC will reduce and hence during the EMI measurement it will show the lower impedance. Zhimin Meng et al [73]developed the multimodal transistor sensor with the help of PZT to explore its thermal and tactile bimodal properties.

Table3: A summary of PZT thin film in energy harvesting application

Structure	Property	Application	Ref.
PZT and polyvinylidene fluoride	Compressive strength	self-powered damage-detection aggregate (SPA)	[74]
PZT and PVDF	Dielectric properties	Piezoelectric Nanogenerator (PEN)	[75]
Yttrium-Iron Garnet (YIG)/TiO_2/PZT	Ferromagnetic resonance (FMR)	spin waves propagation.	[76]

$PbZr_{0.52}Ti_{0.48}O_3$ (PZT) and NiFe2O4 (NFO)	Magnetoelectric coupling	Miniature transducers and sensors	[77]
PZT and oxide thin film transistor (TFT)	Integration of PZT and TFT at low temperature	Micropumps/valves, energy harvesting	[78]
PZT	Conductivity	Sensor	[79]
$CoFe_2O_4$(CFO)/$Pb(Zr_{0.52}Ti_{0.48}O_3)$(PZT)/ $LaNiO_3$(LNO)/NiO	Ferroelectric properties	Magneto electronic devices	[80]
Nb doped PZT film	Presence of internal electric field	Energy harvesting	[81]
Lead zirconate titanate ($Pb(Zr_{0.60}Ti_{0.40})O_3$) thin films.	Dielectric properties	MEMS application	[82]
$PbZr_{0.52}Ti_{0.48}O_3$ nanofibers	dielectric permittivity	Energy storage device	[83]
$Pb(Zr_{0.52}Ti_{0.48})O_3$ (PZT) and relaxor-ferroelectric $Pb_{0.9}La_{0.1}(Zr_{0.52}Ti_{0.48})O_3$ (PLZT) thinfilms are deposited on $SrRuO_3$-covered $SrTiO_3$/Si substrates.	Breakdown strength, remanent polarization, dielectric constant and relaxor ferroelectricity of PLZT	Energy storage based on pulse driving	[84]
Pt/$Pb(Zr_{0.52}Ti_{0.48})O_3$/Pt thin film	Switching of polarization repetitively	Memory devices	[85]
Co/$PbZr_{0.45}Ti_{0.55}O_3$(PZT)/Co	Magnetoelectric effect of the interface	Magnetic memory and sensors	[86]
$Pb(Zr_{0.53}$, $Ti_{0.47})O_3$ (PZT)/$BaTiO_3$ (BTO) bi-layer films	Remnant polarization at room temperature	Energy harvesting and dielectric capacitor	[87]
$Pb(Zr_{0.53}Ti_{0.47})O_3$(PZT) on Pt(111)/TiO2/SiO2/Si substrate	Electric and elastic field coupling	Sensors, transducers and energy harvester	[88]
$Pb(Zr_xTi_{1-x})O_3$ (x=0.20, 0.35, 0.50, 0.52, 0.60, 0.65, and 0.80) thin films on glass substrate	Electro optic properties	Photonic devices	[89]
PZT ($Pb_{0.52}Zr_{0.48}TiO_3$) on LNO ($LaNiO3$) film/silicon substrate	Optical Modulation	Optical field tuned devices or absorbers	[90]
$Pb(Zn_{1/3}Nb_{2/3})O_3$-$Pb(Zr_{1/2}Ti_{1/2})O_3$ (PZN-PZT) and $Pb(In_{1/2}Nb_{1/2})O_3$ (PIN)	Transduction coefficient ($d_{33}\times g_{33}$) and electrostrictive coefficient (Q_{33})	To drive a blue LED and a speed sensor using electrolytic capacitor	[91]
$Pb(Zr_{0.52}Ti_{0.48})O_3$ on glass fiber fabric substrate	Linear change in current/voltage with respect to strain/load	Self-powered nanogenerator	[92]
PZT piezoceramics	Piezoelectric resonance	Micro displacement measurement sensor	[93]
PZT thin film, gandolium (Gd) film and Silicon diaphragm	Thermomagnetic and piezoelectric	AC magnetic field sensor	[94]
Pb0.82Ba0.08La0.1Zr0.9Ti0.1O3 (PBLZT) inorganic thin films	Temperature change with respect to application and removal of electric field	Self-cooling electronic skin	[34]
$PbZr_{0.35}Ti_{0.65}O_3$ thin film on $SrTiO_3$ substrate	Ferroelectric domain structures, topological defects and their conduction	Sensors based on Polarization switch due to applied electric field	[95]
PZT nanoribbon and substrate	Dynamic response	Stretchable electronic	[96]

	to strain	devices	
PZT (d_{31}unimorph structure) and ultra-high vacuum e-beam evaporated (UHVEE) polysilicon	Residual stress and piezoelectric actuation	Micro lens actuator	[97]
$Pb(Zr_{0.52}Ti_{0.48})_{0.95}Nb_{0.05}O_3$ + 0.2 wt.% CeO_2 (PZT-NC)	Dielectric properties (conduction of space charge and relaxation of domain wall)	piezoelectric/ferroelectric devices	[98]
Piezoelectric micromachined ultrasonic trans-ducer (pMUT) on an epitaxial leadzirconate titanate (Epi-PZT) thin film	pMUT ability of transmitting and sensivity of receiving	A finger vessel biometrics	[99]
PZT 5H was used. HBF_4:H_2O=1:10 was used in the etching process.	Etching process was optimized for its rate of etching, selectivity and residue and acid concentration, temperature, and agitation were also kept under control. It has large piezoelectric coefficient.	MEMS applications.	[100]
fiber Bragg grating (FBG) and lead zirconate titanate (PZT) tubes	Optical properties of FBG and piezoelectric properties of PZT.	As a control and protection of smart grid in power system.	[101]
PZT granules $Pb(Zr_{0.52}Ti_{0.48})O_3$ with the doping of MgO by 1.16% and that of Nb_2O_5 by 0.43%	Porosity and permeance of PZT ceramic	Self cleaning PZT membrane for wastewater treatment.	[102]
PZT thin film in metal-ferroelectric-metal (MFM) configuration in 33 mode and exposed with UV rays.	Ferroelectric, single phase and high electrical polarization	Photovoltic application	[103]
PZ29 (Ferroperm Piezoceramics A/S & Meggitt, Denmark) was used with a particle size of 1.3μm. Copolymer P(VDF-TrFE) 56/44 mol.% (Solvay- Solexis, Belgium), was also used.	High piezoelectric coefficient, low permittivity and dielectric losses	Sensors and actuators	[104]
PZT based materials	Piezoelectric properties	Energy harvesting by cardiac activity	[105]
Piezoelectric Energy Harvesting Unit(PEHU)	Natural properties of the PZT i.e., mechanical energy as input and electrical energy as output.	Energy harvesting from highway traffic.	[106]
lead zirconate titanate (PZT) particles and shape memory polyurethane (SMPU) matrix. In addition to that PZT/SMPU nanofibres	Mechanical and thermomechanical properties of PZT and shape memory properties.	Flexible and curved energy harvesting device.	[107]
PZT ceramic patches inside the frame of concrete mix.	Electromechanical properties of PZT.	Dynamic strain sensor as well as an EMI sensor for real time fatigue analysis	[108]
Diamond single point dressing tool and low cost PZT	Electromechanical properties of PZT	Diagnostic system for detection of damage in	[109]

		diamond dressing	
$Pb_{0.99}(Zr_{0.95}Ti_{0.05})_{0.98}Nb_{0.02}O_3$ (PNZT95/5) and $Pb_{0.99}(Zr_{0.95}Ti_{0.05})_{0.98}Nb_{0.02}O_3$ + 1mol% $MnCO_3$ (PNMZT95/5)	Pyroelectric properties and low dielectric constant	Thermal Energy Harvesting	[110]
Unimorph PZT with interdigitated electrode	Increased capacitance	Vibrational Energy Harvesting	[111]
lead zirconate titanate (PZT)-type ceramics doped with Mn^{4+}, Sb^{3+}, W^{6+}, and Ni^{2+}	wide hysteresis loops, high spontaneous polarization, and better values of electromechanical coupling coefficient and the piezoelectric coefficient	Micromechatronic applications	[112]
single-walled carbon nanotube (SWCNT) deposited on PZT/Pt/Ti/SiO2/Si substrates	p-channel transistor characteristics and a clockwise hysteresis loop with high ON/OFF current ratio and large ON current,	Non-volatile memory applications	[113]
PZT/ Polymer composite	High acoustic radiation efficiency and wide frequency bandwidth	As a transducer for measurement of admittance in water and in air.	[114]
Graphene FFETs using single layer grapheme (SLG)/PZT/Pt/SiO2/Si	Enhanced capacitive coupling at gate stack	Memory capacity enhancement	[115]
$Pb(Zr,Ti)O_3$ samples with Zr/Ti ratios: 36/64, 44/56, 52/48, 60/40 and 68/32	Piezoelectric properties, ferroelectric properties, Differential permittivity, energy storage density and dielectric properties	Electronic devices	[116]
PZT particles into a polyvinylidene fluoride (PVDF) matrix	Dielectric properties and Discharged energy density	Dielectric capacitors.	[117]
Nanoparticle based PZT ink and PZT silane film	Dielectric and piezoelectric properties	Vibration energy sensor	[118]

5. Conclusion

This paper has presented the comprehensive study on the PZT material. It has touched upon the various aspects of it. Right from the various methods of fabrication to its applications in different electronic and mechanical products, sensors and actuator have been described. Important properties of the said material have also been elaborated which is paving the way for its numerous applications. Lastly we could say that the PZT thin film is a very promising material and with thrust has been already given to the IoT and Al based products, sensors and actuators the PZT has got a lot more to offer. And it has opened the door of infinite possibility of incorporation of PZT based devices to changing world scenario.

References

1. Y. H. Bing and Z. G. Ye, “Piezo- and ferroelectric (1-x)Pb(Sc1/2Nb1/2)O3-xPbTiO3 solid solution

system," *Handb. Adv. Dielectr. Piezoelectric Ferroelectr. Mater. Synth. Prop. Appl.*, pp. 173–204, 2008.
2. H. Schmid, "Some symmetry aspects of ferroics and single phase multiferroics," *J. Phys. Condens. Matter*, vol. 20, no. 43, 2008.
3. D. Bochenek, P. Niemiec, R. Skulski, M. Adamczyk, and D. Brzezińska, "Electrophysical properties of the multicomponent PBZT-type ceramics doped by Sn 4+," *J. Electroceramics*, vol. 42, no. 1–2, pp. 17–30, 2019.
4. "Title : Multiferroic materials for sensors , transducers and memory devices Author : Zygmunt Surowiak , Dariusz Bochenek Citation style : Surowiak Zygmunt , Bochenek Dariusz . (2008). Multiferroic materials for sensors , transducers and memory devices .," vol. 33, no. 2, 2008.
5. W. Xu, H. L. Huang, Y. Liu, C. Luo, G. Z. Cao, and I. Y. Shen, "Fabrication and characterization of PZT-silane nano-composite thin-film sensors," *Sensors Actuators, A Phys.*, vol. 246, pp. 102–113, 2016.
6. Y. H. Do, M. G. Kang, J. S. Kim, C. Y. Kang, and S. J. Yoon, "Fabrication of flexible device based on PAN-PZT thin films by laser lift-off process," *Sensors Actuators, A Phys.*, vol. 184, pp. 124–127, 2012.
7. K. Terada, T. Suzuki, I. Kanno, and H. Kotera, "Fabrication of single crystal PZT thin films on glass substrates," *Vacuum*, vol. 81, no. 5, pp. 571–578, 2007.
8. M. S. Noh, S. Kim, D. K. Hwang, and C. Y. Kang, "Self-powered flexible touch sensors based on PZT thin films using laser lift-off," *Sensors Actuators, A Phys.*, vol. 261, pp. 288–294, 2017.
9. Z. J. Wang, Y. Aoki, L. J. Yan, H. Kokawa, and R. Maeda, "Crystal structure and microstructure of lead zirconate titanate (PZT) thin films with various Zr/Ti ratios grown by hybrid processing," *J. Cryst. Growth*, vol. 267, no. 1–2, pp. 92–99, 2004.
10. B. Gao *et al.*, "Unexpectedly high piezoelectric response in Sm-doped PZT ceramics beyond the morphotropic phase boundary region," *J. Alloys Compd.*, vol. 836, p. 155474, 2020.
11. N. Kumari *et al.*, "Multifunctional behavior of acceptor-cation substitution at higher doping concentration in PZT ceramics," *Ceram. Int.*, vol. 45, no. 10, pp. 12716–12726, 2019.
12. S. Samanta, V. Sankaranarayanan, and K. Sethupathi, "Effect of Successive Multiple Doping of La, Nb and Fe on Structure and Lattice Vibration of MPB PZT," *Mater. Today Proc.*, vol. 5, no. 14, pp. 27919–27927, 2018.
13. J. Li, P. Li, G. Zhang, J. Yu, Y. Wu, and X. Wen, "The thickness effect of Bi3.25La0.75Ti 3O12 buffer layer in PbZr0.58Ti 0.42O3/Bi3.25La0.75Ti 3O12 (PZT/BLT) multilayered ferroelectric thin films," *Thin Solid Films*, vol. 519, no. 18, pp. 6021–6025, 2011.
14. T. Kobayashi, M. Ichiki, J. Tsaur, and R. Maeda, "Effect of multi-coating process on the orientation and microstructure of lead zirconate titanate (PZT) thin films derived by chemical solution deposition," *Thin Solid Films*, vol. 489, no. 1–2, pp. 74–78, 2005.
15. O. Sugiyama, K. Murakami, and S. Kaneko, "XPS analysis of surface layer of sol-gel-derived PZT thin films," *J. Eur. Ceram. Soc.*, vol. 24, no. 6, pp. 1157–1160, 2004.
16. N. Choudhary, D. K. Kharat, and D. Kaur, "Surface modification of NiTi/PZT heterostructure thin films using various protective layers for potential MEMS applications," *Surf. Coatings Technol.*, vol. 206, no. 7, pp. 1735–1743, 2011.
17. H. Sui, H. Sun, X. Liu, D. Zhou, and R. Xu, "Ferroelectric and dielectric behaviors of sol-gel derived perovskite PMN-PT/PZT heterostructures via compositional development: An interface-dependent study," *J. Eur. Ceram. Soc.*, vol. 38, no. 16, pp. 5382–5387, 2018.
18. M. V. Kamenshchikov, A. V. Solnyshkin, and I. P. Pronin, "Dielectric response of capacitor structures based on PZT annealed at different temperatures," *Phys. Lett. Sect. A Gen. At. Solid State Phys.*, vol. 380, no. 47, pp. 4003–4007, 2016.
19. Z. Jiao, X. Wan, H. Guo, J. Wang, B. Zhao, and M. Wu, "The charge storage characteristics of PZT nanocrystal thin film," *Ultramicroscopy*, vol. 108, no. 10, pp. 1371–1373, 2008.
20. S. Yoshida, H. Hanzawa, K. Wasa, and S. Tanaka, "Enhanced curie temperature and high heat resistivity of PMnN-PZT monocrystalline thin film on Si," *Sensors Actuators, A Phys.*, vol. 251, pp. 100–107, 2016.
21. T. Zhang, W. Li, Y. Yu, M. Wang, J. He, and W. Fei, "Giant electrocaloric effect in compositionally graded PZT multilayer thin films," *J. Alloys Compd.*, vol. 731, pp. 489–495, 2018.
22. A. Bose and M. Sreemany, "Influence of processing conditions on the structure, composition and ferroelectric properties of sputtered PZT thin films on Ti-substrates," *Appl. Surf. Sci.*, vol. 289, pp. 551–559, 2014.
23. R. Wang, E. Tang, G. Yang, and Y. Han, "Experimental research on dynamic response of PZT-5H under impact load," *Ceram. Int.*, vol. 46, no. 3, pp. 2868–2876, 2020.
24. C. Othmani, H. Zhang, and C. Lü, "Effects of initial stresses on guided wave propagation in

multilayered PZT-4/PZT-5A composites: A polynomial expansion approach," *Appl. Math. Model.*, vol. 78, pp. 148–168, 2020.
25. A. Wu, I. M. Miranda Salvado, P. M. Vilarinho, and J. L. Baptista, "Processing and seeding effects on crystallisation of PZT thin films from sol-gel method," *J. Eur. Ceram. Soc.*, vol. 17, no. 12, pp. 1443–1452, 1997.
26. O. Babushkin, T. Lindbäck, K. Brooks, and N. Setter, "PZT phase formation monitored by high-temperature X-ray diffractometry," *J. Eur. Ceram. Soc.*, vol. 17, no. 6, pp. 813–818, 1997.
27. Q. Zou, S. Nourbakhsh, and J. Kim, "Novel polyol-derived sol route for fabrication of PZT thin ferroelectric films," *Mater. Lett.*, vol. 40, no. 5, pp. 240–245, 1999.
28. R. Zuleeg, "Integrated Solgel M Thin-Films on Pt, Si, and Gaas for Non-Volatile Memory Applications," *Ferroelectrics*, vol. 108, no. 1, pp. 37–46, 1990.
29. T. Dufay, B. Guiffard, R. Seveno, S. Ginestar, and J. C. Thomas, "Flexible PZT thin film transferred on polymer substrate," *Surf. Coatings Technol.*, vol. 343, pp. 148–152, 2018.
30. X. Wang *et al.*, "Effect of oxygen partial pressure on crystal quality and electrical properties of RF sputtered PZT thin films under the fixed Ar flow and sputtering pressure," *Vacuum*, vol. 172, p. 109041, 2020.
31. A. Shoghi, H. Abdizadeh, A. Shakeri, and M. R. Golobostanfard, "Sol–gel synthesis of PZT thin films on FTO glass substrates for electro-optic devices," *J. Sol-Gel Sci. Technol.*, vol. 93, no. 3, pp. 623–632, 2020.
32. J. He *et al.*, "Flexible heterogeneous integration of PZT film by controlled spalling technology," *J. Alloys Compd.*, vol. 807, p. 151696, 2019.
33. S. Monga, S. Tomar, P. M. Vilarinho, and A. Singh, "Effect of substrates on optical properties of ferroelectric PZT (52/48) thin films," *Mater. Today Proc.*, no. xxxx, 2020.
34. X. Wang *et al.*, "Enhancements of the electrical properties in Pb1.25(Zr0.52,Ti0.48)O3/Pb1.1(Zr0.52,Ti0.48)O3 ferroelectric multilayered thin films," *Mater. Chem. Phys.*, vol. 241, no. July 2019, p. 122396, 2020.
35. S. T. Kim, J. W. Kim, S. W. Jung, J. S. Shin, S. T. Ahn, and W. J. Lee, "Electrical properties of PZT thin films deposited by electron cyclotron resonance plasma enhanced chemical vapor deposition," *Mater. Chem. Phys.*, vol. 45, no. 2, pp. 155–158, 1996.
36. S. O. Chung, J. W. Kim, S. T. Kim, G. H. Kim, and W. J. Lee, "Microstructure and electric properties of the PZT thin films fabricated by ECR PECVD: The effects of an interfacial layer and rapid thermal annealing," *Mater. Chem. Phys.*, vol. 53, no. 1, pp. 60–66, 1998.
37. J. M. Koo, S. Kim, S. Shin, Y. Park, and J. K. Lee, "Influence of purge gas on the characteristics of lead-zirconium-titanate thin films prepared by metalorganic chemical vapor deposition," *Ceram. Int.*, vol. 34, no. 4, pp. 1003–1006, 2008.
38. W. G. Lee and Y. J. Kwon, "Preparation of ferroelectric PZT thin films by plasma enhanced chemical vapor deposition using metalorganic precursors," *J. Ind. Eng. Chem.*, vol. 14, no. 1, pp. 89–93, 2008.
39. G. He, Y. Zhang, C. Peng, and X. Li, "Surface morphology and ferroelectric properties of compositional gradient PZT thin films prepared by chemical solution deposition process," *Appl. Surf. Sci.*, vol. 283, pp. 532–536, 2013.
40. E. H. Kim, C. W. Moon, J. G. Lee, M. S. Lah, and S. M. Koo, "Synthesis and characterization of lead (IV) precursors and their conversion to PZT materials through a CVD process," *Polyhedron*, vol. 177, p. 114270, 2020.
41. P. Muralt *et al.*, "Fabrication and characterization of PZT thin-film vibrators for micromotors," *"Sensors and Actuators, A: Physical,"* vol. 48, no. 2. pp. 157–165, 1995.
42. T. Hata, S. Kawagoe, W. Zhang, K. Sasaki, and Y. Yoshioka, "Proposal of new mixture target for PZT thin films by reactive sputtering," *Vacuum*, vol. 51, no. 4, pp. 665–671, 1998.
43. M. Watamori *et al.*, "Ion beam analysis of PZT thin films," *Appl. Surf. Sci.*, vol. 142, no. 1, pp. 422–427, 1999.
44. X. S. Li, K. Yamashita, T. Tanaka, Y. Suzuki, and M. Okuyama, "Structural and electrical properties of highly oriented Pb(Zr,Ti)O3 thin films deposited by facing target sputtering," *Sensors Actuators, A Phys.*, vol. 82, no. 1, pp. 265–269, 2000.
45. Y. C. Lin, H. A. Chuang, and J. H. Shen, "PZT thin film preparation by pulsed DC magnetron sputtering," *Vacuum*, vol. 83, no. 6, pp. 921–926, 2009.
46. K. K. Maurya, S. K. Halder, S. Sen, A. Bose, and S. Bysakh, "High resolution X-ray and electron microscopy characterization of PZT thin films prepared by RF magnetron sputtering," *Appl. Surf. Sci.*, vol. 313, pp. 196–206, 2014.
47. S. Choi, J. Park, J. Kang, A. T. C. Johnson, and Y. C. Kang, "Surface characterization of PZT thin films obtained at various O2 gas ratios," *Vacuum*, vol. 128, pp. 234–239, 2016.
48. M. Akhtari Zavareh, B. Abd Razak, M. H. Bin Wahab, B. T. Goh, R. Mahmoodian, and K. Wasa,

"Fabrication of Pb(Zr,Ti)O3 thin films utilizing unconventional powder magnetron sputtering (PMS)," *Ceram. Int.*, vol. 46, no. 2, pp. 1281–1296, 2020.
49. L. H. Hamedi, M. Guilloux-Viry, A. Perrin, and M. H. Cherkani, "On the epitaxial growth of PZT films by pulsed laser deposition," *Ann. Chim. Sci. des Mater.*, vol. 23, no. 1–2, pp. 377–380, 1998.
50. J. R. Gatabi *et al.*, "Tuning electrical properties of PZT film deposited by Pulsed Laser Deposition," *Ceram. Int.*, vol. 43, no. 8, pp. 6008–6012, 2017.
51. M. Botea *et al.*, "Structural, electric and pyroelectric properties of up and down graded PZT multilayers," *Curr. Appl. Phys.*, vol. 19, no. 7, pp. 804–810, 2019.
52. J. Jeon and K. H. Kim, "Evolution of domain structure in PbZr0.52Ti0.48O3 thin film by adding dysprosium," *Thin Solid Films*, vol. 701, p. 137940, 2020.
53. N. Godard, S. Glinsek, and E. Defay, "Inkjet-printed silver as alternative top electrode for lead zirconate titanate thin films," *J. Alloys Compd.*, vol. 783, pp. 801–805, 2019.
54. I. Fraile, M. Gabilondo, N. Burgos, M. Azcona, and F. Castro, "Laser sintered ceramic coatings of PZT nanoparticles deposited by Inkjet Printing on metallic and ceramic substrates," *Ceram. Int.*, vol. 44, no. 13, pp. 15603–15610, 2018.
55. S. P. Bathurst and S. G. Kim, "Printing of uniform PZT thin films for MEMS applications," *CIRP Ann. - Manuf. Technol.*, vol. 62, no. 1, pp. 227–230, 2013.
56. D. Gong, F. Qin, Y. Wang, Y. Chen, T. Yang, and X. Sun, "Adjustable response of PZT thin film based piezoelectric micro-actuator through DC bias pre-polarization," *Solid. State. Electron.*, vol. 163, no. October 2019, p. 107675, 2020.
57. X. Wang *et al.*, "Orientation transition, dielectric, and ferroelectric behaviors of sol-gel derived PZT thin films deposited on Ti–Pt alloy layers: A Ti content-dependent study," *Ceram. Int.*, vol. 46, no. 8, pp. 10256–10261, 2020.
58. H. Dong, M. Chen, H. Zhu, Y. Huang, Q. Ding, and J. Feng, "Effects of thermal strain on electric properties of lead zirconate titanate thin films upon LaNiO3 coated base metal plates," *Ceram. Int.*, vol. 46, no. 2, pp. 1883–1887, 2020.
59. K. T. Arul and M. S. R. Rao, "Ferroelectric properties of flexible PZT composite films," *J. Phys. Chem. Solids*, p. 109371, 2020.
60. M. D. Nguyen, "Impact of fatigue behavior on energy storage performance in dielectric thin-film capacitors," *J. Eur. Ceram. Soc.*, vol. 40, no. 5, pp. 1886–1895, 2020.
61. B. Cherdhirunkorn, S. Surakulananta, J. Tangsritrakul, D. Hall, and S. Intarasiri, "The effect of nitrogen ion implantation on the physical and dielectric properties of cobalt-doped PZT ceramics," *Results Phys.*, vol. 16, no. December 2019, p. 102851, 2020.
62. L. Li *et al.*, "Epitaxial growth of full range of compositions of (1 1 1) PbZr1-xTixO3 on GaN," *J. Cryst. Growth*, vol. 538, 2020.
63. Q. Zhang *et al.*, "Effect of electrode interfaces on peak-drift switching current of PZT thin films," *Ceram. Int.*, vol. 45, no. 3, pp. 3159–3165, 2019.
64. M. K. Bhattarai, K. K. Mishra, A. A. Instan, B. P. Bastakoti, and R. S. Katiyar, "Enhanced energy storage density in Sc3+ substituted Pb(Zr0.53Ti0.47)O3 nanoscale films by pulse laser deposition technique," *Appl. Surf. Sci.*, vol. 490, no. March, pp. 451–459, 2019.
65. H. Mao *et al.*, "PZT/Ti composite piezoceramic membranes for liquid filtration: Fabrication and self-cleaning properties," *J. Memb. Sci.*, vol. 581, no. October 2018, pp. 28–37, 2019.
66. H. Wang, M. Godara, Z. Chen, and H. Xie, "A one-step residue-free wet etching process of ceramic PZT for piezoelectric transducers," *Sensors Actuators, A Phys.*, vol. 290, pp. 130–136, 2019.
67. M. C. Chun, S. Park, S. Park, G. yeon Park, and B. S. Kang, "Effects of Pb content and electrode materials on the ferroelectric properties of Pb(Zr0.52Ti0.48)O3 thin films," *J. Alloys Compd.*, vol. 781, pp. 1028–1032, 2019.
68. S. H. Wankhade, S. Tiwari, A. Gaur, and P. Maiti, "PVDF–PZT nanohybrid based nanogenerator for energy harvesting applications," *Energy Reports*, vol. 6, pp. 358–364, 2020.
69. N. Chamankar, R. Khajavi, A. A. Yousefi, A. Rashidi, and F. Golestanifard, "A flexible piezoelectric pressure sensor based on PVDF nanocomposite fibers doped with PZT particles for energy harvesting applications," *Ceram. Int.*, 2020.
70. M. Rezaei and R. Talebitooti, "Wideband PZT energy harvesting from the wake of a bluff body in varying flow speeds," *Int. J. Mech. Sci.*, vol. 163, no. June, 2019.
71. Y. Lu, J. Chen, Z. Cheng, and S. Zhang, "The PZT/Ni unimorph magnetoelectric energy harvester for wireless sensing applications," *Energy Convers. Manag.*, vol. 200, no. June, p. 112084, 2019.
72. W. Li, T. Liu, D. Zou, J. Wang, and T. H. Yi, "PZT based smart corrosion coupon using electromechanical impedance," *Mech. Syst. Signal Process.*, vol. 129, pp. 455–469, 2019.
73. Z. Meng *et al.*, "Lead Zirconate Titanate (a piezoelectric ceramic)-Based thermal and tactile bimodal organic transistor sensors," *Org. Electron.*, vol. 80, no. January, p. 105673, 2020.

74. X. Ji, Y. Hou, Y. Chen, and Y. Zhen, "Fabrication and performance of a self-powered damage-detection aggregate for asphalt pavement," *Mater. Des.*, vol. 179, p. 107890, 2019.
75. M. Koç, L. Paralı, and O. Şan, "Fabrication and vibrational energy harvesting characterization of flexible piezoelectric nanogenerator (PEN) based on PVDF/PZT," *Polym. Test.*, p. 106695, 2020.
76. S. A. Sharko *et al.*, "Ferromagnetic and FMR properties of the YIG/TiO2/PZT structures obtained by ion-beam sputtering," *J. Magn. Magn. Mater.*, p. 167099, 2020.
77. L. Jian, A. S. Kumar, C. S. C. Lekha, S. Vivek, and I. Salvado, "Nano-Structures & Nano-Objects Strong sub-resonance magnetoelectric coupling in PZT-NiFe 2 O 4 -PZT thin film composite," *Nano-Structures & Nano-Objects*, vol. 18, p. 100272, 2019.
78. P. Trong, R. Shimura, T. Shimoda, and Y. Takamura, "Sensors and Actuators A : Physical Direct integration of piezoactuator array with active-matrix oxide thin-film transistors using a low-temperature solution process," *Sensors Actuators A. Phys.*, vol. 295, pp. 125–132, 2019.
79. B. D. Zaitsev, A. P. Semyonov, A. A. Teplykh, and I. A. Borodina, "The e ff ect of the conductivity of a fi lm located near a piezoelectric resonator with a lateral electric fi eld based on the PZT ceramics on its characteristics," no. September, 2018.
80. S. Meenachisundaram, H. Mori, and T. Kawaguchi, "Magnetoelectric effect in free-standing multiferroic thin fi lm," *J. Alloys Compd.*, vol. 787, pp. 1128–1135, 2019.
81. C. Su, K. Liu, J. Ho, D. Heon, and Y. Soo, "Internal- fi eld-dependent low-frequency piezoelectric energy harvesting characteristics of in situ processed Nb-doped Pb (Zr , Ti) O 3 thin- fi lm cantilevers," *J. Alloys Compd.*, vol. 781, pp. 898–903, 2019.
82. X. Wang *et al.*, "Enhanced dielectric and piezoelectric properties of RF sputtered Pb (Zr 0 . 60 , Ti 0 . 40) O 3 thin fi lms deposited on sol-gel derived Pb 1 þ x (Zr 0 . 40 , Ti 0 . 60) O 3 seed layer with various lead contents," *J. Alloys Compd.*, vol. 807, p. 151660, 2019.
83. Y. Zhang *et al.*, "Optimizing the dielectric energy storage performance in P (VDF-HFP) nanocomposite by modulating the diameter of PZT nanofibers prepared via electrospinning," vol. 184, no. August, 2019.
84. M. D. Nguyen, C. T. Q. Nguyen, H. N. Vu, and G. Rijnders, "Experimental evidence of breakdown strength and its e ff ect on energy- storage performance in normal and relaxor ferroelectric fi lms," *Curr. Appl. Phys.*, vol. 19, no. 9, pp. 1040–1045, 2019.
85. M. C. Chun, S. Park, S. Park, G. Park, and B. S. Kang, "E ff ects of repetitive polarization switching on the coercive voltage of Pt / Pb (Zr 0 . 52 Ti 0 . 48) O 3 / Pt thin fi lms analyzed using impedance spectroscopy," *Curr. Appl. Phys.*, vol. 19, no. 4, pp. 503–505, 2019.
86. S. A. Sharko, A. I. Serokurova, N. N. Novitskii, V. A. Ketsko, and A. I. Stognij, "Continuous ferrimagnetic Y3Fe5O12 layers on the ceramic PbZr0.45Ti0.55O3 substrates," *Ceram. Int.*, pp. 0–27, 2020.
87. Y. Wang, J. Yan, H. Cheng, N. Chen, P. Yan, and F. Yang, "Lead zirconate titanate and barium titanate bi-layer ferroelectric fi lms on Si," *Ceram. Int.*, vol. 45, no. 7, pp. 9032–9037, 2019.
88. A. Matavˇ, T. Rojac, and B. Maliˇ, "Self-assembled porous ferroelectric thin films with a greatly enhanced piezoelectric response z Bradeˇ," vol. 16, pp. 83–89, 2019.
89. M. Zhu, H. Zhang, Z. Du, and C. Liu, "Structural insight into the optical and electro-optic properties of lead zirconate titanate for high-performance photonic devices," *Ceram. Int.*, no. July, pp. 0–1, 2019.
90. Y. Zeng, F. Ling, and J. Yao, "substrate in the terahertz region," vol. 88, no. September 2018, pp. 621–624, 2019.
91. J. Yan, Y. Hou, X. Yu, M. Zheng, and M. Zhu, "Journal of the European Ceramic Society Large enhancement of transduction coe ffi cient in PZN-PZT energy harvesting system through introducing low- ε r PIN relaxor," *J. Eur. Ceram. Soc.*, vol. 39, no. 8, pp. 2666–2672, 2019.
92. S. He, W. Dong, Y. Guo, L. Guan, H. Xiao, and H. Liu, "Nano Energy Piezoelectric thin fi lm on glass fi ber fabric with structural hierarchy : An approach to high-performance , super fl exible , cost-e ff ective , and large-scale nanogenerators," vol. 59, no. March, pp. 745–753, 2019.
93. B. D. Zaitsev, A. P. Semyonov, A. A. Teplykh, and I. A. Borodina, "The sensor for measuring the micro-displacements based on the piezoelectric resonator with lateral electric field," *Ultrasonics*, vol. 99, no. April, p. 105973, 2019.
94. C. Chen, I. Chen, H. Duan, C. Tseng, and T. Chung, "Sensors and Actuators A : Physical A thermomagnetic-piezoelectric MEMS AC magnetic-field sensor demonstrating a novel room-temperature-range coil-less resetting / demagnetizing approach," *Sensors Actuators A. Phys.*, vol. 297, p. 111509, 2019.
95. S. Mo *et al.*, "Superdomain structure and high conductivity at the vertices in the (111) - oriented epitaxial tetragonal Pb (Zr , Ti) O 3 thin fi lm," *Curr. Appl. Phys.*, vol. 19, no. 4, pp. 418–423, 2019.
96. B. Wang, H. Bi, H. Ouyang, Y. Wang, and Z. Deng, "Dynamic behaviour of piezoelectric nanoribbons with wavy configurations on an elastomeric substrate," *Int. J. Mech. Sci.*, p. 105787, 2020.

97. S. Chen, A. Michael, and C. Y. Kwok, "actuator with residual stress control," *Sensors Actuators A. Phys.*, no. xxxx, p. 111620, 2019.
98. Y. Chen, H. Zhou, S. Wang, Q. Chen, and Q. Wang, "Diffused phase transition, ionic conduction mechanisms and electric-field dependent ferroelectricity of Nb/Ce co-doped Pb(Zr0.52Ti0.48)O3 ceramics," *J. Alloys Compd.*, p. 155500, 2020.
99. Z. Liu, S. Yoshida, T. Horie, S. Okamoto, and R. Takayama, "Sensors and Actuators A : Physical Feasibility study of ultrasonic biometrics based on finger vessel imaging by epitaxial-PZT / Si piezoelectric micromachined ultrasonic transducer," *Sensors Actuators A. Phys.*, vol. 312, p. 112145, 2020.
100. H. Wang, M. Godara, Z. Chen, and H. Xie, "Sensors and Actuators A : Physical A one-step residue-free wet etching process of ceramic PZT for piezoelectric transducers," *Sensors Actuators A. Phys.*, vol. 290, pp. 130–136, 2019.
101. Y. He, Q. Yang, S. Sun, M. Luo, R. Liu, and G. Peng, "Electrical Power and Energy Systems A multi-point voltage sensing system based on PZT and FBG," *Electr. Power Energy Syst.*, vol. 117, no. February 2019, p. 105607, 2020.
102. H. Mao *et al.*, "Journal of the European Ceramic Society High-performance self-cleaning piezoelectric membrane integrated with in- situ ultrasound for wastewater treatment," *J. Eur. Ceram. Soc.*, vol. 40, no. 10, pp. 3632–3641, 2020.
103. R. Gupta, V. Gupta, and M. Tomar, "Ferroelectric PZT thin films for photovoltaic application," *Mater. Sci. Semicond. Process.*, vol. 105, no. March 2019, 2020.
104. T. Siponkoski, M. Sc, M. Nelo, H. Jantunen, and J. Juuti, "A printable P (VDF-TrFE) -PZT Composite with Very High Piezoelectric Coefficient," vol. 20, 2020.
105. L. Dong *et al.*, "Cardiac energy harvesting and sensing based on piezoelectric and triboelectric designs," *Nano Energy*, p. 105076, 2020.
106. C. Chen, A. Sharafi, and J. Sun, "A high density piezoelectric energy harvesting device from highway traffic – Design analysis and laboratory validation," *Appl. Energy*, vol. 269, no. April, p. 115073, 2020.
107. X. Guan, H. Chen, H. Xia, Y. Fu, J. Yao, and Q. Ni, "Flexible energy harvester based on aligned PZT / SMPU nanofibers and shape memory effect for curved sensors," *Compos. Part B*, vol. 197, no. May, p. 108169, 2020.
108. M. Haq, S. Bhalla, and T. Naqvi, "Fatigue damage monitoring of reinforced concrete frames using wavelet transform energy of PZT-based admittance signals," *Measurement*, vol. 164, p. 108033, 2020.
109. P. Cirp *et al.*, "ScienceDirect ScienceDirect ScienceDirect Damage patterns recognition in dressing tools using PZT-based SHM and MLP networks A new methodology to analyze the functional MLP existing products for an assembly oriented product family identification CIRP Desi," *Procedia CIRP*, vol. 79, pp. 303–307, 2018.
110. X. Chen, S. Yan, H. Nie, F. Cao, G. Wang, and X. Dong, "Improved pyroelectric fi gures of merit of Mn-doped Zr-rich lead zirconate titanate bulk ceramics near room temperature for energy harvesting applications," *J. Alloys Compd.*, vol. 779, pp. 450–455, 2019.
111. M. Lee, C. Kim, W. Park, J. Cho, and J. Paik, "Energy harvesting performance of unimorph piezoelectric cantilever generator using interdigitated electrode lead zirconate titanate laminate," *Energy*, vol. 179, pp. 373–382, 2019.
112. D. Bochenek, P. Niemiec, R. Skulski, and M. Adamczyk-habrajska, "Journal of Physics and Chemistry of Solids Electrophysical properties of a multicomponent PZT-type ceramics for actuator applications," *J. Phys. Chem. Solids*, vol. 133, no. November 2018, pp. 128–134, 2019.
113. Y. Sun, D. Xie, R. Dai, M. Sun, W. Li, and T. Ren, "Ferroelectric polarization effect on hysteresis behaviors of single- walled carbon nanotube network fi eld-effect transistors with lead zirconate-titanate gating," *Curr. Appl. Phys.*, vol. 18, no. 3, pp. 324–328, 2018.
114. Y. Hwang, H. Ahn, D. Nguyen, W. Kim, and W. Moon, "Sensors and Actuators A : Physical An underwater parametric array source transducer composed of PZT / thin-polymer composite," *Sensors Actuators A. Phys.*, vol. 279, pp. 601–616, 2018.
115. S. Lee and Y. Lee, "Graphene / lead-zirconate-titanate ferroelectric memory devices with tenacious retention characteristics," *Carbon N. Y.*, vol. 126, pp. 176–182, 2018.
116. S. Samanta, V. Sankaranarayanan, and K. Sethupathi, "Band gap , piezoelectricity and temperature dependence of di ff erential permittivity and energy storage density of PZT with di ff erent Zr / Ti ratios," *Vacuum*, vol. 156, no. May, pp. 456–462, 2018.
117. G. Chen, X. Lin, J. Li, J. G. Fisher, Y. Zhang, and S. Huang, "Enhanced dielectric properties and discharged energy density of composite fi lms using submicron PZT particles," *Ceram. Int.*, vol. 44, no. 13, pp. 15331–15337, 2018.
118. W. Xu, H. Huang, Y. Liu, C. Luo, G. Z. Cao, and I. Y. Shen, "Sensors and Actuators A : Physical Fabrication and characterization of PZT-silane nano-composite thin-film sensors," *Sensors Actuators*

A. Phys., vol. 246, pp. 102–113, 2016.

119. Chitte, P., Rathod, S., Motgi, N., Jangale, Y., & Patil, R. (2018). Design and Fabrication of Automated Pneumatic Shearing Machine to Cut Aluminium Sheet". International Journal of Mechanical and Production Engineering Research and Development, p-ISSN (2018), 2249, 6890.
120. Wannasuth, S. (2015). The Increase in Synergy's Value of Supply Chain's Triangle Corners for Retail Business. BEST: International Journal of Management, Information Technology and Engineering (BEST: IJMITE), 3(12), 1-6.
121. Yogesh, M., Chandramohan, G., & Vishruth, P. Innovations in Manufacturing Systems and Technologies for Global Competitiveness: A Context of Lean Manufacturing. BEST: International Journal of Management, Information Technology and Engineering (BEST: IJMITE), 3(10), 43-52.
122. Reddy, S., & Dufera, S. (2016). Additive Manufacturing Technologies. Best: International Journals of Management, Information Technology and Engineering (BEST: IJMITE), ISSN (P), 2348-0513.
123. Hassan, M. U., & Singh, S. (2016). Fabrication, Experimentation, Performance Evaluation of Two Stage Air Cooler and Comparison with Conventional Air Cooler. International Journal of Mechanical Engineering (IJME), 5(4), 75-84.
124. YUN, K., KONG, J., YANASE, S., & OKUMIYA, M. NEW FABRICATION METHOD SUGGESTION OF THE MOTOR CORE WITH DISSIMILAR METAL BONDING METHOD.
125. Santhosh, M. S., Sasikumar, R., Natrayan, L., Kumar, M. S., Elango, V., & Vanmathi, M. (2018). Investigation of mechanical and electrical properties of Kevlar/E-glass and Basalt/E-glass reinforced hybrid composites. International Journal of Mechanical and Production Engineering Research and Development, 8(3), 591-598.